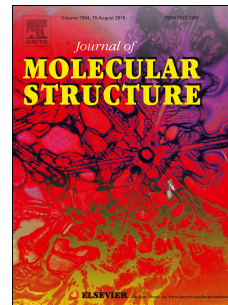


# Journal Pre-proof

Synthesis and characterization of a new class of phenothiazine molecules with 10H-substituted morpholine & piperidine derivatives: A structural insight

Javeena Hussain, Deekshi Angira, Tanya Hans, Pankaj Dubey, Sivapriya Kirubakaran, Vijay Thiruvengatam



PII: S0022-2860(20)30871-1

DOI: <https://doi.org/10.1016/j.molstruc.2020.128546>

Reference: MOLSTR 128546

To appear in: *Journal of Molecular Structure*

Received Date: 23 April 2020

Revised Date: 25 May 2020

Accepted Date: 26 May 2020

Please cite this article as: J. Hussain, D. Angira, T. Hans, P. Dubey, S. Kirubakaran, V. Thiruvengatam, Synthesis and characterization of a new class of phenothiazine molecules with 10H-substituted morpholine & piperidine derivatives: A structural insight, *Journal of Molecular Structure* (2020), doi: <https://doi.org/10.1016/j.molstruc.2020.128546>.

This is a PDF file of an article that has undergone enhancements after acceptance, such as the addition of a cover page and metadata, and formatting for readability, but it is not yet the definitive version of record. This version will undergo additional copyediting, typesetting and review before it is published in its final form, but we are providing this version to give early visibility of the article. Please note that, during the production process, errors may be discovered which could affect the content, and all legal disclaimers that apply to the journal pertain.

© 2020 Published by Elsevier B.V.

### Credit Author Statement

**Javeena Hussain (JH):** Synthesized all the molecules, Crystallized the molecules and writing-original draft preparation, **Deekshi Angira (DA):** Crystallographic analysis and writing of the manuscript, **Tanya Hans (TH):** Synthesized the molecules **Pankaj Dubey (PD):** DFT calculation and analysis, **Sivapriya Kirubakaran (SK):** Idea of synthesis of the new class of phenothiazine molecules with morpholine substitution and proof reading of the manuscript, **Vijay Thiruvakatam (VT):** Conceptualization the idea, designed the manuscript contents and crystallographic data analysis and curation.

## Synthesis and characterization of a new class of phenothiazine molecules with 10H-substituted morpholine & piperidine derivatives: A structural insight

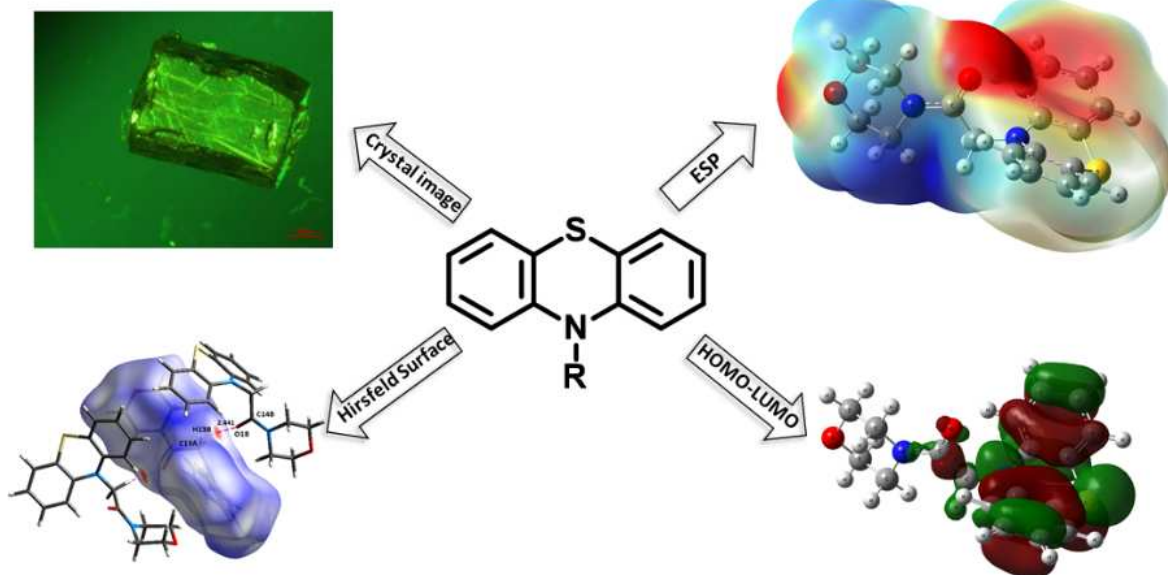
Javeena Hussain<sup>1</sup>, Deekshi Angira<sup>1</sup>, Tanya Hans<sup>1</sup>, Pankaj Dubey<sup>1</sup>, Sivapriya Kirubakaran<sup>1</sup> and Vijay Thiruvengadam<sup>2, \*</sup>

<sup>1</sup> Discipline of Chemistry, Indian Institute of Technology Gandhinagar, Gandhinagar, Gujarat-382355, India

<sup>2</sup> Discipline of Biological Engineering, Indian Institute of Technology Gandhinagar, Gandhinagar, Gujarat-382355, India

E-mail: [vijay@iitgn.ac.in](mailto:vijay@iitgn.ac.in)

### Graphical abstract:



## Synthesis and characterization of a new class of phenothiazine molecules with 10H-substituted morpholine & piperidine derivatives: A structural insight

Javeena Hussain<sup>1</sup>, Deekshi Angira<sup>1</sup>, Tanya Hans<sup>1</sup>, Pankaj Dubey<sup>1</sup>, Sivapriya Kirubakaran<sup>1</sup> and Vijay Thiruvengatam<sup>2, \*</sup>

<sup>1</sup> Discipline of Chemistry, Indian Institute of Technology Gandhinagar, Gandhinagar, Gujarat-382355, India

<sup>2</sup> Discipline of Biological Engineering, Indian Institute of Technology Gandhinagar, Gandhinagar, Gujarat-382355, India

\*E-mail: [vijay@iitgn.ac.in](mailto:vijay@iitgn.ac.in)

### Abstract:

A series of 10H-substituted phenothiazine-based molecules were prepared by the base-catalyzed reactions. The synthesized compounds are characterized by Mass spectroscopy, NMR, and SCXRD to examine the role of different functional groups involved in the intermolecular interactions and conformational geometries. The crystal packing of the compounds is governed by O–H...O, C–H...O, and  $\pi$ – $\pi$  interactions. A complete understanding of the intermolecular interactions is studied employing the Hirshfeld analysis, 2D Fingerprint plot. Furthermore, the density functional theory (DFT/B3LYP) method at the 6–311++G(d,p) basis set was performed to support and compare experimental & theoretical geometrical parameters of phenothiazine derivatives.

**Keywords:** Phenothiazine, Crystal packing, Hirshfeld, 2D Fingerprint plot, DFT, HOMO-LUMO

### Introduction:

The investigation of 10H substituted phenothiazine derivatives has steadily grown fast because they exhibit a wide range of applications in medicinal chemistry. Phenothiazine moiety is present in a wide range of synthetic compounds and is considered as one of the most important ‘privileged substructures’ because of the wide spectrum of biological activities displayed by many of its derivatives. It is the parent molecule of a significant series of drugs called the major tranquilizers.<sup>1</sup> The crystallographic elucidation of the structures of phenothiazine and some of the derivatives was initiated in McDowell’s laboratory.<sup>2</sup> Bernthsen<sup>3</sup> was the first one who synthesized phenothiazine called thiodiphenylamine in 1883 during the proof of structural studies of dyes such as methylene blue. Later, it has played an important function in dye chemistry.<sup>4</sup> Phenothiazine and its derivatives have found several applications in other fields also,

and this has inspired further study on these compounds. These are heterocyclic molecules containing two benzene rings connected in a tricyclic system through nitrogen and sulfur atom. The slight change in substitution in the phenothiazine nucleus causes a distinguishable difference in their biological activities. Phenothiazine related structures are building blocks for many drugs that have shown diverse biological activities such as insecticidal<sup>5</sup> properties in 1934; further work demonstrated its usefulness as an antiseptic<sup>6</sup> and an antihelmintic.<sup>7</sup> Its derivatives have been particularly valuable in human medicine as antihistamines<sup>8</sup> in the treatment of Parkinson's disease<sup>9</sup>, and as antimalarial<sup>10</sup>, antipsychotic<sup>11</sup>, antimicrobial<sup>12, 13</sup> antitubercular<sup>14</sup>, antitumor<sup>15</sup>, antifungal<sup>16</sup>, and antioxidants.<sup>17</sup> Due to the increased importance of these heterocyclic compounds, several attempts were made during the past few years in the synthesis of a new generation of 10H substituted phenothiazine's scaffolds that exert a wide range of biological effects.<sup>18</sup> Together with their psychotic effects, other biological effects such as cancer chemotherapy were very well documented.<sup>19</sup> The mechanisms of these effects have been previously well known and related to the chemical structure of derivatives synthesized from the phenothiazine family. The presence of intermolecular interactions and the conformational geometry implemented by the molecules influence the level of biological activity.<sup>20-22</sup>

To examine the function of different functional groups engaged in the intermolecular interactions and conformational geometries, a series of five 10H substituted phenothiazine derivatives have been synthesized, crystallized, and studied for their structural feature. Adding to the list of next-generation of 10H-substituted phenothiazine's derivatives, we report the synthesis and analytical characterization of the compounds along with structural analysis via single-crystal X-ray diffraction and DFT calculation of the morpholine and piperidine based phenothiazine scaffolds, 2-(10H-phenothiazine-10-yl)-1-(piperidine-1-yl) ethanone (**2a**), 1-morpholino-2-(10H-phenothiazine-10-yl) ethanone (**2b**), 2-bromo-1-(10H-phenothiazine-10-yl) ethanone (**3**), 1-(10H-phenothiazine-10-yl)-2-(piperidine-1-yl) ethanone (**3a**) and 2-morpholino-1-(10H-phenothiazin-10-yl) ethanone (**3b**) (**Figure 1**). Here, we report the new phenothiazine derivatives of pharmacological interest, which are attractive scaffolds in terms of biological studies and would be the part of numerous important therapeutic applications.

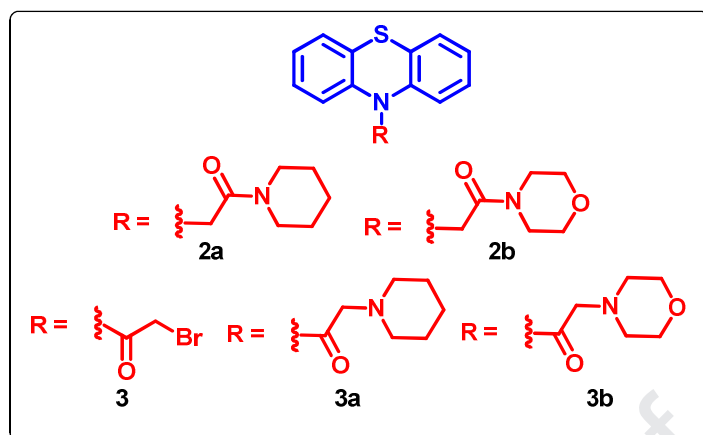


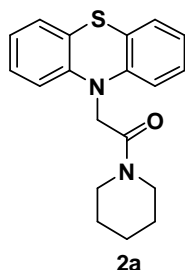
Figure 1. Different variations of the R group.

## Experimental

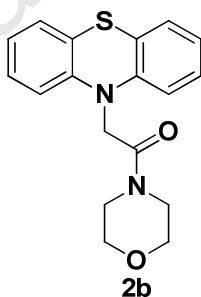
### General Considerations for the synthesis of all the 5 compounds

All the chemicals were of analytical grade procured from Sigma, Merck, Finar, and SD Fine. The reaction was done in a round-bottomed flask with a Teflon-coated and magnetic stirring bar under inert condition. The monitoring of the progress of the reactions was done by Thin-layer chromatography (TLC) carried on Merck TLC silica gel 60 F254 and visualized by ultraviolet irradiation. Infrared (IR) spectra were performed on a Perkin Elmer FTIR Spectrometer Spectrum 2 and absorption bands were reported in wavenumbers ( $\text{cm}^{-1}$ ). The mass spectrums of all the synthesized compounds were obtained by Waters Synapt-G2S ESI-Q-TOF Mass instrument in the positive mode. The NMR of the synthesized compounds was recorded on Bruker AVANCE III 500 ( $^1\text{H}$ NMR: 500 MHz,  $^{13}\text{C}$ NMR: 125 MHz). Melting points (mp) for solid compounds were recorded using LAB INDIA Visual Melting Range Apparatus (MR-Vis) instrument in an open glass capillary.

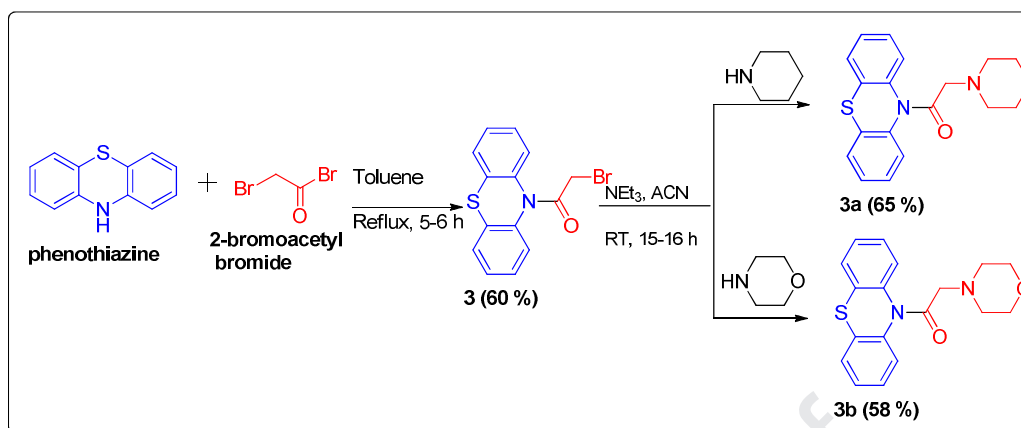


**2-(10H-phenothiazin-10-yl)-1-(piperidin-1-yl) ethanone, 2a**

Yield (78 mg , ~ 47 %) ; mp -196 – 198 °C; IR ( $\nu$ ,  $\text{cm}^{-1}$ ): 1651 (C=O), 1220 (C–N);  $^1\text{H}$  NMR (500 MHz, chloroform-*d*):  $\delta$  7.1 (d,  $J = 7.5$  Hz, 4H), 6.9 (t,  $J = 7.3$  Hz, 2H), 6.7 (d,  $J = 8.0$  Hz, 2H), 4.5 (s, 2H), 3.6 (t,  $J = 5.5$  Hz, 2H), 3.5 (d,  $J = 4.9$  Hz, 2H), 1.6 (m, 4H), 1.5 (m, 2H);  $^{13}\text{C}$  NMR (125 MHz, chloroform-*d*):  $\delta$  166.05, 144.56, 127.41, 127.00, 123.98, 122.91, 115.23, 53.43, 52.11, 46.48, 43.48, 29.72, 26.61, 25.71, 24.46; ESI-MS:  $m/z$ , calculated for  $\text{C}_{19}\text{H}_{21}\text{N}_2\text{OS}$   $[\text{M}+\text{H}]^+$  325.13, found: 325.11.

**1-morpholino-2-(10H-phenothiazin-10-yl) ethanone, 2b**

Yield (70 mg , ~ 42%); mp-194 – 196 °C ; IR ( $\nu$ ,  $\text{cm}^{-1}$ ): 1648 (C=O), 1232 (C–N), 1112 (C–O);  $^1\text{H}$  NMR (500 MHz, chloroform-*d*):  $\delta$  7.1 (m, 4H), 6.9 (m, 2H), 6.8 (d,  $J = 9.3$  Hz, 2H), 4.5 (s, 2H), 3.5 (m, 8H);  $^{13}\text{C}$  NMR (125 MHz, chloroform-*d*):  $\delta$  166.50, 144.31, 127.53, 127.32, 124.55, 123.31, 115.30, 66.91, 66.86, 46.04, 42.72. ESI-MS:  $m/z$ , calculated for  $\text{C}_{18}\text{H}_{19}\text{N}_2\text{O}_2\text{S}$   $[\text{M}+\text{H}]^+$  327.11, found: 327.12.

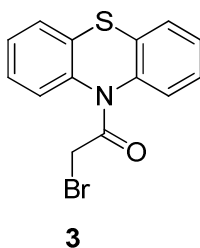


Scheme 2. Synthetic route of **3**, **3a**, and **3b**.

### Synthesis of **3**, (2-bromo-1-(10H-phenothiazine-10-yl) ethanone)

To a solution of phenothiazine (200 mg, 1 mmol) in toluene, 2-bromoacetyl bromide (201.84 mg, 1.00 mmol) was added slowly under the inert condition at 0-5 °C. The reaction mixture was refluxed at 120-130 °C for 5-6 h, the progress of the reaction was monitored by TLC. Then the solution was diluted with ethyl acetate and washed with brine. The organic layer was dried over Na<sub>2</sub>SO<sub>4</sub> and evaporated on a rotary evaporator at 45-50 °C and the crude product was purified by silica gel column chromatography (5 % ethyl acetate: Hexane) to yield **3**.

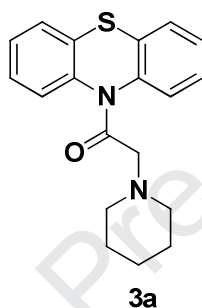
### 2-bromo-1-(10H-phenothiazin-10-yl)ethanone, **3**



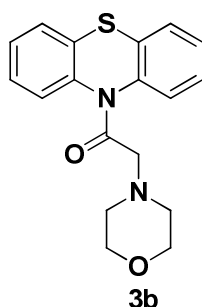
Yield (194 mg, ~ 60 %) ; mp-128 – 130 °C; IR (ν, cm<sup>-1</sup>): 1666(C=O), 698(C–Br); <sup>1</sup>H NMR (500 MHz, chloroform-*d*): δ 7.5 (d, *J* = 8.0 Hz, 2H), 7.4 (d, *J* = 7.5 Hz, 2H), 7.3 (t, *J* = 8.0 Hz, 2H), 7.2 (t, *J* = 7.5 Hz, 2H), 3.93 (s, 2H); <sup>13</sup>CNMR (125 MHz, chloroform-*d*): δ 164.73, 137.10, 127.10, 126.36, 126.26, 125.48, 25.87; ESI-MS: *m/z*, calculated for C<sub>14</sub>H<sub>11</sub>BrNOS [M+2H]<sup>+</sup> 321.99, found: 321.96.

**Synthesis of 3a and 3b**

To a solution of piperidine or morpholine (3 eq.) was taken in a dry round-bottomed flask in dichloromethane and triethylamine,  $\text{NEt}_3$  (2 eq.) was added. Followed by the addition of **3** (1 eq.) at room temperature and the reaction mixture was stirred for 15-16 h. After completion, the reaction mixture was diluted with ethyl acetate and washed with water. The organic layer was dried over  $\text{Na}_2\text{SO}_4$  and evaporated on a rotary evaporator at 45-50 °C. The crude product was purified by silica gel column chromatography (5-10 % ethyl acetate: Hexane) to get **3a** and **3b** as pure solid.

**1-(10H-phenothiazin-10-yl)-2-(piperidin-1-yl) ethanone, 3a**

Yield (133 mg, ~ 65 %); mp-156 – 158 °C; IR ( $\nu$ ,  $\text{cm}^{-1}$ ): 1668 (C=O), 1260 (C–N);  $^1\text{H}$  NMR (500 MHz, chloroform-*d*):  $\delta$  7.5 (d,  $J = 7.9$  Hz, 2H), 7.4 (dd,  $J = 6.5$  Hz, 2H), 7.3 (m, 2H), 7.3 (m, 2H), 3.2 (s, 2H), 2.3 (m, 4H), 1.5 (m, 4H), 1.3 (m, 2H);  $^{13}\text{C}$  NMR (125 MHz, chloroform-*d*):  $\delta$  169.16, 138.93, 127.82, 126.67, 61.17, 54.10, 25.94, 23.89; ESI-MS:  $m/z$ , calculated for  $\text{C}_{19}\text{H}_{21}\text{N}_2\text{OS}$   $[\text{M}+\text{H}]^+$  325.13, found: 325.21.

**2-morpholino-1-(10H-phenothiazin-10-yl) ethanone, 3b**

Yield ~ 58 %; mp-132 – 134 °C; IR ( $\nu$ ,  $\text{cm}^{-1}$ ): 1678 (C=O), 1262 (C–N), 1115 (C–O);  $^1\text{H}$  NMR (500 MHz, chloroform-*d*)  $\delta$  7.55 (d,  $J = 7.9$  Hz, 2H), 7.45 (d,  $J = 7.8$  Hz, 2H), 7.34 – 7.29 (m, 2H), 7.25 – 7.21 (m, 2H), 3.58 (t,  $J = 4.7$  Hz, 4H), 3.30 (s, 2H), 2.42 (t,  $J = 4.7$  Hz, 4H);  $^{13}\text{C}$  NMR

(125 MHz, chloroform-*d*)  $\delta$  168.48, 138.79, 127.91, 126.93, 126.83, 126.74, 66.85, 60.71, 53.26.  
ESI-MS:  $m/z$ , calculated for C<sub>18</sub>H<sub>19</sub>N<sub>2</sub>O<sub>2</sub>S: [M+H]<sup>+</sup> 327.11, found: 327.07.

### Crystallographic analysis

The characterization and quantification of the intermolecular interactions in these molecules were carried out by the Hirshfeld surface(HS) analysis and 2D (two-dimensional) fingerprint plots using the Crystal Explorer program<sup>23, 24</sup>. The HS was mapped with  $d_{\text{norm}}$ , shape index, and curvedness, which helps to reveal the intermolecular interactions and the crystal packing. The 2D fingerprint plots give a measurement of the different intermolecular interactions.<sup>25</sup>

**Crystallization:** The saturated solutions of newly synthesized compounds **2a**, **2b**, **3**, **3a**, and **3b** were prepared in appropriate solvents. The solutions were allowed for solvent evaporation in a dust-free environment. The crystals were obtained in dichloromethane and tertiary butyl methyl ether solvents (1:1) at ambient temperature using the slow evaporation method. The good quality crystals were harvested and subjected to single-crystal X-ray diffraction analysis.

### Single crystal X-ray diffraction data

The data were collected from a single crystal at 150/273/293 K on Bruker APEX-II CCD using Mo K $\alpha$  ( $\lambda = 0.7107 \text{ \AA}$ ). All the crystal structures were solved using *SHELXS97*<sup>26</sup> refined using *SHELXL2014*<sup>27</sup> and reduced by the full-matrix least-squares method using Bruker *SAINT*. Molecular graphics were generated using Bruker *SHELXTL* and packing diagrams were generated using Mercury CSD 4.0.0.<sup>28</sup> The non-hydrogen atoms are refined anisotropically and the hydrogen atoms bonded to C atoms were positioned geometrically and refined using a riding model with distance restraints C—H = 0.93–0.98  $\text{\AA}$  with  $U_{\text{iso}}(\text{H}) = 1.2U_{\text{eq}}(\text{Csp}^2)$  or  $1.5U_{\text{eq}}(\text{Csp}^3)$ .

**Table 1.** Crystal data and structure refinement for the **2a**, **2b**, **3**, **3a**, and **3b**.

	<b>2a</b>	<b>2b</b>	<b>3</b>	<b>3a</b>	<b>3b</b>
<b>Crystal data</b>					
<b>Chemical formula</b>	C <sub>19</sub> H <sub>20</sub> N <sub>2</sub> OS	C <sub>18</sub> H <sub>18</sub> N <sub>2</sub> O <sub>2</sub> S	C <sub>14</sub> H <sub>10</sub> BrNOS	C <sub>19</sub> H <sub>20</sub> N <sub>2</sub> OS	C <sub>18</sub> H <sub>18</sub> N <sub>2</sub> O <sub>2</sub> S
<b>CCDC number</b>	1918910	1918911	1884801	1918908	1953850
<b>M<sub>r</sub></b>	324.43	326.40	320.19	324.43	326.40

<b>Crystal system, space group</b>	Monoclinic, $P2_1/n$	Monoclinic, $P2_1/n$	Orthorhombic, $Pca2_1$	Monoclinic, $P2_1/c$	Monoclinic, $P2_1/c$
<b>Temperature (K)</b>	273	273	150	273	293
<b><math>a, b, c</math> (Å)</b>	15.2521 (10), 9.7811 (6), 23.6183 (17)	13.155 (3), 15.606 (4), 15.836 (4)	10.8958 (13), 8.9037 (12), 26.023 (3)	15.5041 (4), 9.0491 (2), 12.7418 (3)	15.073 (10), 9.100 (3), 12.724 (8)
<b><math>\alpha, \beta, \gamma</math> (°)</b>	90, 104.906 (3), 90	90, 105.271 (6), 90	90, 90, 90	90, 109.228 (1), 90	90, 107.94 (3), 90
<b><math>V</math> (Å<sup>3</sup>)</b>	3404.9 (4)	3136.3 (13)	2524.5 (5)	1687.93 (7)	1660.4 (16)
<b><math>Z</math></b>	8	8	8	4	4
<b>Radiation type</b>	Mo $K\alpha$	Mo $K\alpha$	Mo $K\alpha$	Mo $K\alpha$	Mo $K\alpha$
<b><math>\mu</math> (mm<sup>-1</sup>)</b>	0.20	0.22	3.41	0.20	0.21
<b>Crystal size (mm)</b>	0.30 × 0.20 × 0.10	0.30 × 0.10 × 0.01	0.18 × 0.17 × 0.14	0.40 × 0.20 × 0.10	0.1 × 0.05 × 0.03
<b>Data collection</b>					
<b>Diffractometer</b>	Bruker APEX-II CCD	Bruker APEX-II CCD	Bruker APEX-II CCD	Bruker APEX-II CCD	Bruker SMART APEX2 CCD area detector
<b>Absorption correction</b>	Multi-scan	Multi-scan	Multi-scan	Multi-scan	Multi-scan
<b><math>T_{\min}, T_{\max}</math></b>	0.684, 0.746	0.53, 1.00	0.543, 0.623	0.91, 0.98	0.632, 0.746
<b>No. of measured, independent and observed reflections</b>	17632, 10166, 4769 [ $I > 2\sigma(I)$ ]	34041, 9585, 5191 [ $I > 2\sigma(I)$ ]	31834, 6282, 5684 [ $I \geq 2u(I)$ ]	12520, 4136, 3633 [ $I > 2\sigma(I)$ ]	12833, 4072, 3103 [ $I > 2\sigma(I)$ ]
<b><math>R_{\text{int}}</math></b>	0.039	0.060	0.049	0.022	0.048
<b><math>(\sin \theta/\lambda)_{\text{max}}</math> (Å<sup>-1</sup>)</b>	0.715	0.719	0.667	0.667	0.666
<b>Refinement</b>					
<b><math>R[F^2 &gt; 2\sigma(F^2)], wR(F^2), S</math></b>	0.067, 0.216, 0.99	0.054, 0.188, 1.01	0.025, 0.050, 1.00	0.040, 0.151, 1.21	0.047, 0.164, 1.07
<b>No. of reflections</b>	10166	9585	6244	4136	4072
<b>No. of parameters</b>	415	415	405	208	208
<b>H-atom treatment</b>	H-atom parameters constrained	H-atom parameters constrained	All H-atom parameters refined	H-atom parameters constrained	H-atom parameters constrained

$\Delta_{\text{max}}, \Delta_{\text{min}} (\text{e} \text{ \AA}^{-3})$	0.29, -0.37	0.32, -0.44	0.27, -0.38	0.26, -0.23	0.26, -0.24
--	-------------	-------------	-------------	-------------	-------------

### Cambridge structure database search

The Cambridge structure database<sup>29, 30</sup> searches was carried out using ConQuest version 2.0.0<sup>31</sup> with **2a**, **2b**, **3**, **3a**, and **3b** together with alkyl-substituted phenothiazine moiety to understand the similarities, packing arrangement and dominant interactions in these kinds of chemical compounds.

### Hirshfeld surface analysis

The Crystal explorer software used to estimate the strength of contacts by analyzing the interaction energies and evaluate these facts with the outputs of the Hirshfeld surface analysis. Properties like curvedness, shape index, and  $d_{\text{norm}}$  were studied for all the four compounds. The relative contribution of various contacts present in the individual crystal was plotted with respect to their respective 2D decomposition plots.<sup>24, 25, 32, 33</sup>

### Powder X-ray diffraction (PXRD)

All the synthesized compounds were characterized by X-ray diffraction employing a Bruker D8 Discover diffractometer with  $\text{CuK}\alpha$  radiation. The PXRD patterns were recorded in a  $2\theta$  range of 5 to 90° with a step size of 0.02 and at a scanning rate of 0.2 second per step. The tube voltage and current were 20 kV and 5 mA, respectively. The intense and sharp patterns of PXRD of all compounds confirmed good crystalline properties.

## Results and discussion

### Chemistry

The synthesis of new derivatives of piperidine and morpholine bearing alkyl chains of the same lengths, connected to the N atom of the heterocyclic system of phenothiazine was accomplished in good or moderate yields by advancing and modifying usual procedures reported in the literature. Compounds **2a**, **2b**, **3**, **3a**, and **3b** were synthesized by reacting **1a** and **1b** with phenothiazine<sup>34</sup> in the presence of sodium hydride (NaH) as a base and N, N-dimethylformamide (DMF) as a solvent (**Scheme 1**). Another three compounds were synthesized by the acetylation of the phenothiazine using appropriate halogen alkyl reagent. Bromo-acetyl bromide in toluene was refluxed with 10H-phenothiazine; it afforded the corresponding 10-bromo acetyl phenothiazine

(3). To prepare 10H-substituted phenothiazine amine derivative compounds, the morpholine and piperidine were selected for this synthetic approach (**Scheme 2.**) The reaction of 10-bromo acetyl phenothiazine (**3**) with morpholine and piperidine substituents, took place at room temperature in dry acetonitrile (ACN), in the presence of trimethylamine ( $\text{NEt}_3$ ) as a base gave the corresponding products **3a** and **3b**. The structures of all the compounds were confirmed by their  $^1\text{H}$  NMR,  $^{13}\text{C}$  NMR, and Mass spectrum.

### Structure description

An extensive CSD survey was performed to understand the similarities and conformational changes of the title compounds. There are no reports of the structures similar to the compounds **2a**, **2b**, **3**, **3a**, and **3b** in the crystal database. However, there was one hit DUBZUV4<sup>35</sup> for alkyl-substituted phenothiazine moiety with few similarities concerning the puckered conformation of the bent phenyl rings, typical to the chemical compounds under study.

ORTEP<sup>36</sup> and capped stick diagrams for compounds **2a**, **2b**, **3**, **3a** and **3b** are displayed in the **supplementary figure S1** and **figure S2** respectively. The compounds **2a**, **2b**, **3a**, and **3b** crystallize in the centrosymmetric monoclinic system with **2a** and **2b** having a  $P2_1/n$  space group and **3a** and **3b** having  $P2_1/c$  space group. The compound **3** crystallizes in the orthorhombic system and depicts  $Pca2_1$ . The compounds **2a** and **2b** are solved and refined as a dimer. The asymmetric unit is composed of two molecules with the molecular formula  $\text{C}_{19}\text{H}_{20}\text{N}_2\text{OS}$  and  $\text{C}_{18}\text{H}_{18}\text{N}_2\text{O}_2\text{S}$  for **2a** and **2b** respectively. Both the compounds have a Z value of 8. Their structures exhibit 'T shaped' morphology with phenothiazine ring plane located perpendicular to the piperidine moiety. The molecular conformation of **2a** is stabilized by C...H and O...H contacts as seen in the packing diagram whereas in **2b** the major driving interactions are O...H and S---H contacts.

The compound **3a** and **3b** with the molecular formula of  $\text{C}_{19}\text{H}_{20}\text{N}_2\text{OS}$  and  $\text{C}_{18}\text{H}_{18}\text{N}_2\text{O}_2\text{S}$  are solved as a monomer with one molecule in the asymmetric unit and Z value of 4. Their structure displays a slight difference with 'crooked T shape' morphology where the piperidine moiety is bent over the phenothiazine ring with the amide linker showing a torsion angle  $\text{N1}\dots\text{C13}\dots\text{C14}\dots\text{N2}$  of  $-65.53^\circ$  for **3a** and  $-62.11^\circ$  for **3b**. The packing is assisted by O...H interactions playing the master role in both the cases.

The compound **3** is solved as a dimer with the molecular formula,  $C_{14}H_{10}BrNOS$  with 2 molecules in the asymmetric unit, and a Z value of 8. Unlike compounds **2a**, **2b**, **3a**, and **3b**, this compound comprises of bromo acetyl moiety connected to phenothiazine via amide linker. The major contacts participating in the packing of this derivative include O...H, S...H, and Br...Br contacts.

One of the interesting features that we can notice in all these compounds is the folded butterfly-like<sup>37</sup> phenothiazine ring moiety that has a characteristic bent along the N-S vector and the dihedral angle between two planes lie in a range of 132-142° that is again distinctive feature for phenothiazine derivatives.<sup>1, 35</sup> Also, as discussed in by McDowell in<sup>1</sup>, the N and the S atoms are located at a considerable distance from the two planes and are not exactly located at the axis where the two planes intersect. As shown in the **figure. 2**, the distance calculated for **2a** is 0.002 Å (N) and 0.206 Å (S), for **2b** it is 0.041 Å (N) and 0.293 Å (S), for **3a** it is 0.022 Å (N), and 0.050 Å (S), for **3b** it is 0.076 Å (N) and 0.117 Å (S) and for **3** it is 0.076 Å (N) and 0.030 Å (S).

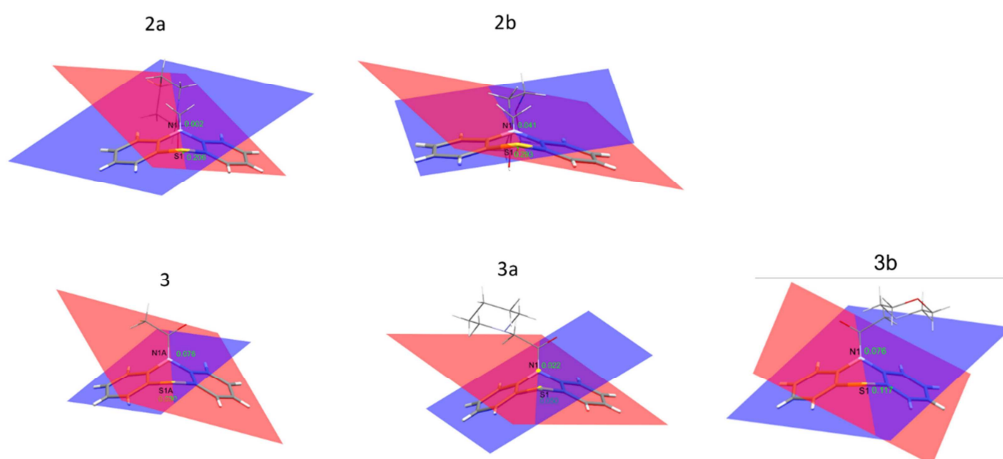


**Figure 2.** Representation of plane angles of **2a**, **2b**, **3**, **3a**, and **3b**.

### Hirshfeld surface analysis

The structure files for all the five compounds in the CIF format were submitted in Crystal Explorer software to generate the Hirshfeld surface (HS) as shown in **figure 3**. It encodes for the intermolecular interactions based on the electron density map of the molecule for the electron density of its neighboring molecule. The  $d_{\text{norm}}$  was mapped in the range of -0.227 to 1.401, shape index was mapped in the range of -1.00 to 1.00, and curvedness had a range of -4.00 to 0.40 for

all the compounds. The intense red spots are indicating the places where the intermolecular distances are shorter than the sum of van der Waals radii.<sup>38,39</sup> Also, the quantitative breakdown of the intermolecular contacts is also analyzed using the 2D fingerprint plots generated using  $d_i$  versus  $d_e$  values. The blue, white, and red color contacts utilized for the  $d_{\text{norm}}$  mapped Hirshfeld surfaces distinguish the interatomic conventions as longer, at van der Waals partitions and small interatomic contacts, correspondingly<sup>40</sup>. We can see the strong C—H...O interactions as bright red spots between the relevant donor and acceptor atoms on the Hirshfeld surfaces mapped over  $d_{\text{norm}}$  (**Figure 3**).

The HS analysis of compound **2a** depicted the presence of a strong hydrogen bond, C14-O1...H13B-C13, between oxygen (amide linker of one molecule) and hydrogen (amide linker of the neighboring molecule) with a bond distance of 2.129 Å. The compound **2b**, which has a carbon substituted with oxygen in the morpholine moiety did not illustrate much difference and showed S1...H1-C1 (2.740 Å) in addition to the C14-O1...H13B-C13 (2.304 Å) hydrogen bond in the form of electron-rich red spots on the molecular surface. On the other hand, in compound **3a**, major interactions were C13-O1...H9-C9, C13-O1...H2-C2, and C1-H1...C11 with the bond distance of 2.353 Å, 2.478 Å, and 2.763 Å respectively. Likewise, compound **3b** also showed C13-O1...H9-C9 and C13-O1...H2-C2 contact with the bond distance of 2.679 Å, and 2.523 Å respectively. Owing to the presence of bromo acetyl moiety, compound **3** shows a strong Br...Br interaction between the two monomers with a bond distance of 3.346 Å. The  $\theta_1$ (C14A-Br1A...Br1B) and  $\theta_2$  (C14B-Br1B...Br1A) angles for the interaction are calculated as 145.5 ° and 161.7 ° respectively, thereby confirming this contact as quasi-type 1 halogen-halogen interaction.<sup>41</sup> A hydrogen bond between C14A-H14a...O1B with a bond distance of 2.454 Å was also present in compound **3**. The fingerprint or the decomposition plot for all the title compounds is given in **figure 4**. Based on the fingerprint plots, a table for the percentage contribution of major interactions is highlighted in **table 2**.

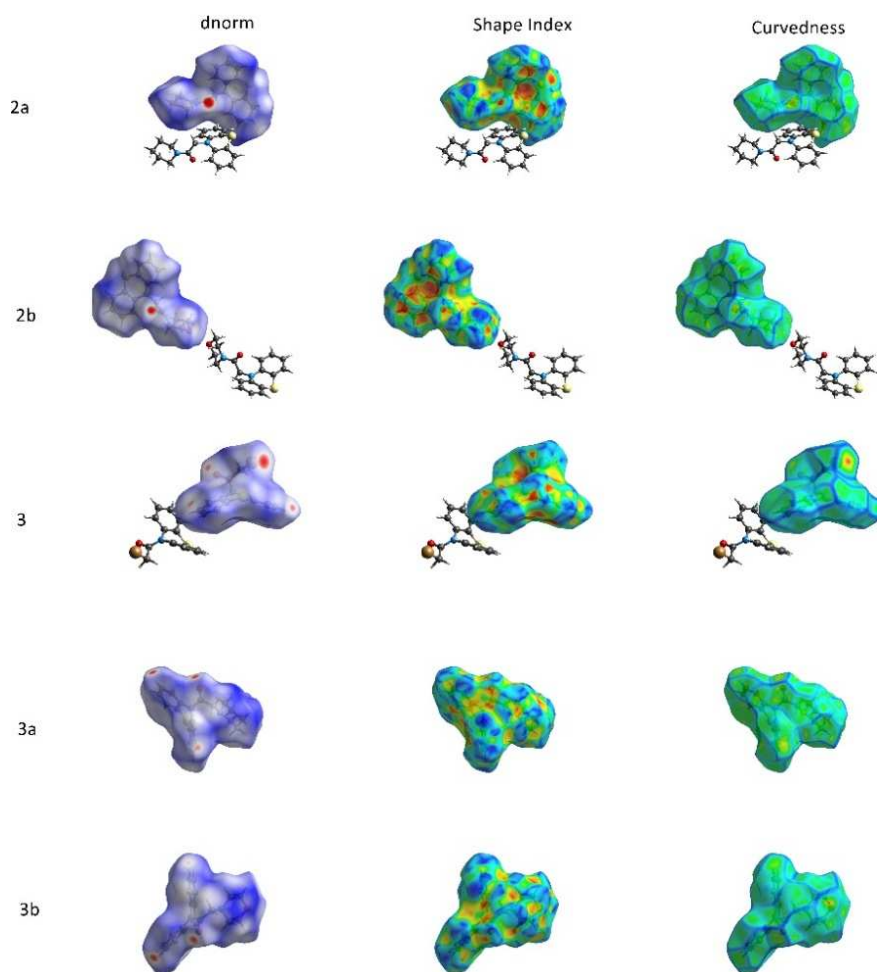


**Figure 3.** Hirshfeld surfaces of **2a**, **2b**, **3**, **3a**, and **3b** mapped with (a) *dnorm*, (b) shape index, and (c) curvedness.

The valuable measures of Hirshfeld surfaces mapped over shape-index and curvedness, commenced by Koendrink<sup>42</sup> and offer additional chemical insight into molecular packing. A surface with low curvedness assigns a flat area and may be indicative of  $\pi$ - $\pi$  stacking interactions in the crystal.<sup>43</sup> The occurrence of the  $\pi$ - $\pi$  stacking interactions is also specified by the emergence of red and blue spots on the shape indexed surfaces, documented and in the flat areas on the Hirshfeld surfaces mapped with curvedness in **Figure 3**. The curvedness map showed green flat areas and the shape index has corresponding red (negative) and blue (positive) spots such as triangles, which are discrete for the identification of  $\pi$ - $\pi$  stacking. Further, the intermolecular interactions in the morpholine/piperidine attached derivatives of phenothiazine

are analyzed by the 2D fingerprint plot. It has been generated from the Hirshfeld surface analysis illustrate the percentage contacts of strong and weak intermolecular interactions on the compounds. The 2D fingerprint plot offered the frequency of each intermolecular interaction take place in the crystal (**Table 2**).

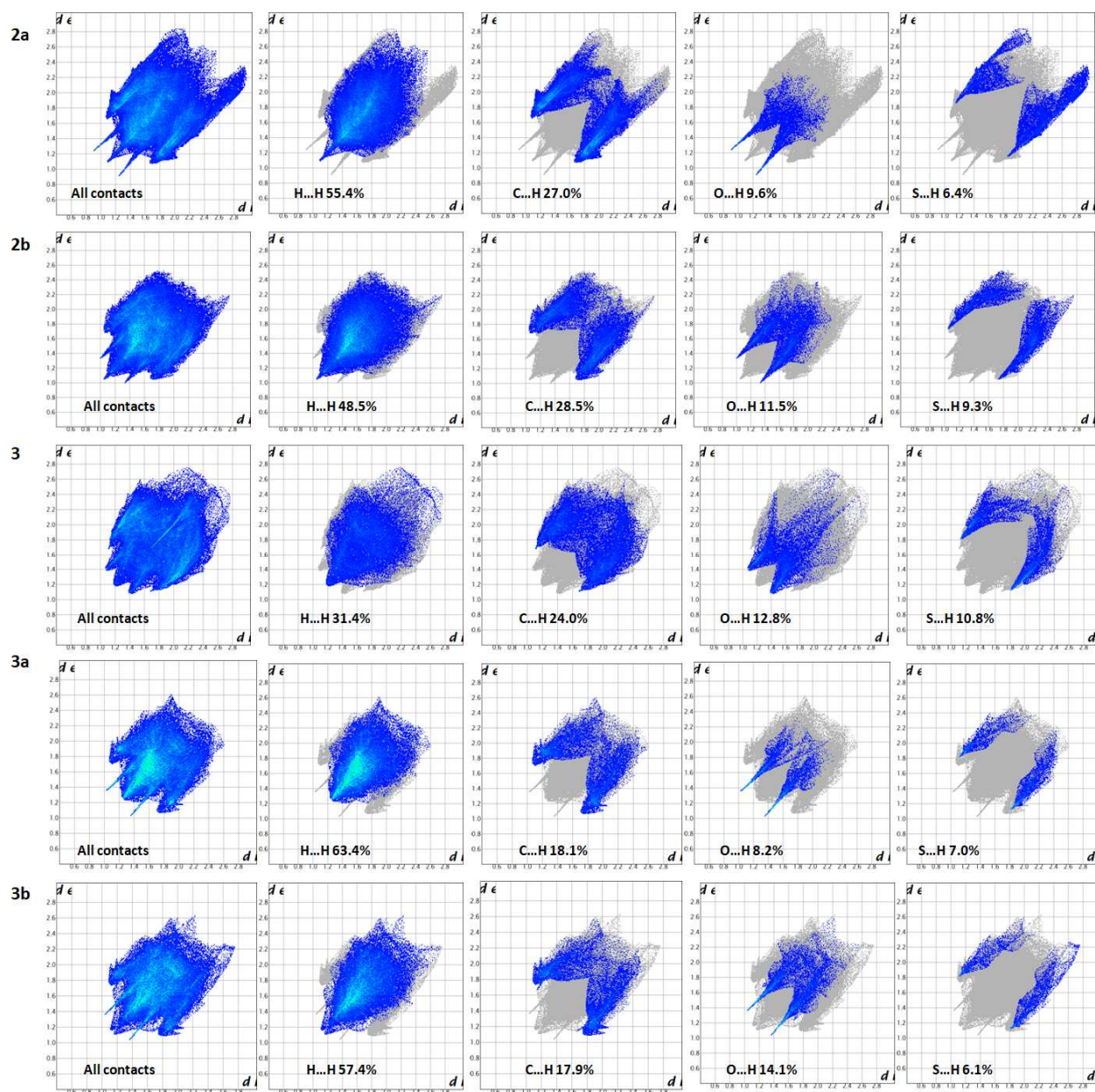


**Figure 4.** The two-dimensional fingerprint plot analysis of **2a**, **2b**, **3**, **3a**, and **3b** (a) all interactions, (b) HH contacts (c) CH contacts (c) OH contacts and (c) SH contacts.

According to the data, 0.2 to 3.3 percent of C...C contacts also confirms the presence of  $\pi$ - $\pi$  stacking in all the calculated system (Supplementary, **Figure S14**). The main intermolecular

interactions influencing the molecular packing of the studied phenothiazine derivatives are the C–H...O and H...H and  $\pi$ – $\pi$  interactions (**Table 2**). We can notice that in compound **2a**, the maximum contribution is from H...H contacts i.e. 55.4% followed by C...H, S...H, and O...H with values of 27%, 9.6%, and 6.4% respectively. A similar pattern was observed in **2b** with the H...H, C...H, O...H, and S...H contacts having the percentage contribution of 48.5%, 28.5%, 11.5%, and 9.3% respectively. The presence of oxygen in the morpholine moiety of **2b** is majorly responsible for the increase in O...H contact contribution and a concomitant decrease in H...H contribution when compared to **2a**. The compound **3a**, which is very similar to **2a** and differs only with respect to the position of oxygen in amide linker surprisingly, displays a different pattern of contact contribution, hence, highlighting the importance of the position of functional group and its effect in intermolecular interaction.

**Table 2.** The relative contribution of different close contacts for the overall intermolecular interactions in 10H substituted phenothiazine derivatives.

Contacts	Compounds				
	2a	2b	3	3a	3b
H...H (%)	55.4	48.5	29.6	63.3	57.4
C...H (%)	27.0	28.5	29.7	18.1	17.9
O...H (%)	9.6	11.5	11.9	8.2	14.1
S...H (%)	6.4	9.3	9.8	7.0	6.1
C...C (%)	0.2	1.5	0.5	3.0	3.3
Br...H (%)	-	-	11.8	-	-

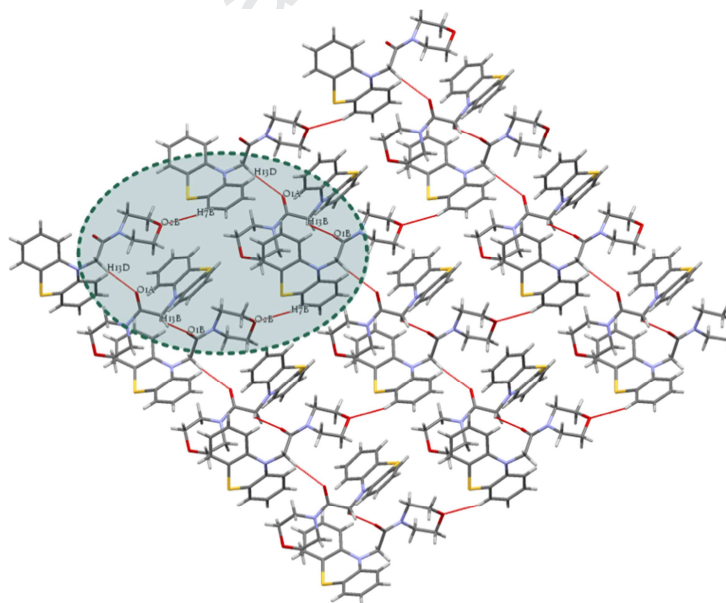
The H...H contributes to 63.3%, highest among all the four derivatives, followed by C...H, O...H, and S...H with values of 18.1%, 8.2%, and 7% respectively. Compound **3b**, which is again similar to the **2b**, has maximum contact contribution from H...H (57.4%) followed by C...H (17.9%), O...H (14.1%), and S...H (6.1%). The slight increase in O...H contact contribution can be owed to the presence of two oxygen atoms, in amide linker and morpholine moiety respectively. Similarly, in compound **3**, the presence of bromo acetyl moiety is accountable for 11.8% Br...H and 2.3% Br...Br contacts in addition to the contribution by H...H, C...H, O...H and S...H of 29.6%, 29.7%, 11.9%, and 9.8% respectively. A drastic decrease in H...H contact contribution is noticed in **3**, due to the structural difference as compared to other derivatives.

**Table 3.** Selected Hydrogen bond parameters (Å, °) of **2a**, **2b**, **3**, **3a**, and **3b**

Compound	<i>D</i> — <i>H</i> ··· <i>A</i>	<i>D</i> — <i>H</i> (Å)	<i>H</i> ··· <i>A</i> (Å)	<i>D</i> ··· <i>A</i> (Å)
<b>2a</b>	C13A—H13B···O1A <sup>a</sup>	0.97	2.26	3.217 (2)
	C13B—H13C···O1B <sup>b</sup>	0.97	2.24	3.207 (2)
<b>2b</b>	C4B—H4B···S1A <sup>c</sup>	0.93	2.87	3.700 (2)
	C13A—H13B···O1B	0.97	2.44	3.143 (3)
	C13B—H13D···O1A <sup>d</sup>	0.97	2.41	3.374 (2)
<b>3</b>	C1A—H1A···S1A <sup>e</sup>	0.95	2.95	3.747 (3)
	C10A—H10A···Br1A	0.95	2.95	3.608 (4)
	C14B—H14C···O1A <sup>f</sup>	0.99	2.58	3.511 (4)
<b>3a</b>	C2—H2···O1 <sup>g</sup>	0.93	2.50	3.404(2)
<b>3b</b>	C2—H2···O1 <sup>g</sup>	0.93	2.25	3.424(3)

Symmetry code(s): (a)  $-x+1/2, y+1/2, -z+3/2$ ; (b)  $-x+3/2, y-1/2, -z+3/2$ ; (c)  $x-1/2, -y+3/2, z+1/2$ ; (d)  $x-1/2, -y+3/2, z-1/2$ ; (e)  $x-1/2, -y+1, z$ ; (f)  $-x+3/2, y, z-1/2$ ; (g)  $-x, 1-y, -z$ ;

After analyzing the CIF for all the compounds, significant formation of supramolecular assemblies was observed in compounds **2a**, **3a**, and **3b**. As seen in compound **2b** (**Figure 5**), a supramolecular synthon formation occurs utilizing 3 dimers (6 molecules) linked to each other by hydrogen bonds, thus, forming an elliptical cavity in a two-dimensional arrangement. The bond formation occurs between C13B-H13D...O1A, C13A-H13B...O1B, C7B-H7B...O2B with the bond distance of 2.41 Å, 2.44 Å, and 2.67 Å respectively.

**Figure 5.** Crystal packing diagram depicting supramolecular synthon formation in compound **2b** in a unit cell viewed down the, *b* direction

In Compound **3a** and **3b**, a similar synthon formation occurs in the form of a zig-zag herringbone pattern utilizing hydrogen bond being formed between C2-H2...O1 with a bond distance of 2.50 Å in 3A and 2.25 Å in 3B. Both of the herringbone chains run parallel to each other this holding the molecules together as shown in **Figure 6**.

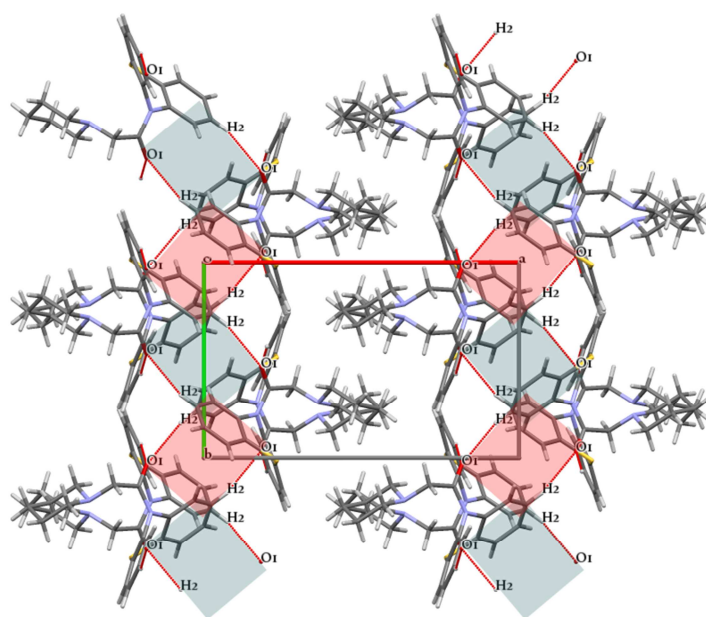


**Figure 6.** Supramolecular structure formation of compound **3a** in a unit cell viewed along the *b* direction

### Density functional theory

The electronic structure calculations were performed at the DFTB3LYP level of theory employing a 6-311++G(d,p) basis set. The theoretical calculations were carried out using the Gaussian 09 program<sup>44</sup> and visualized in GaussView program.<sup>45</sup> Previous reports suggest that the nature of electron density distribution around molecule and its reactivity can be understood in terms highest occupied molecular orbital (HOMO) and lowest unoccupied molecular orbital (LUMO).<sup>46</sup> Furthermore, it is also stated that the molecular regions with the high density of the HOMO determine the site for electrophilic attacks. Whereas, the region for the nucleophilic attack is governed by the high density of the LUMO.<sup>47</sup> The stability and reactivity of the molecule can be understood in terms of the energy differences between HOMO and LUMO.<sup>48,49</sup>

**Figure 7** shows optimized geometry, HOMO, and LUMO of the 10H substituted derivatives of Phenothiazine, and **Table 4** shows the absolute energy, dipole moment, HOMO energy, LUMO energy and gap between HOMO and LUMO orbitals, for all five derivatives of phenothiazine. The

HOMO and LUMO of all the compounds were plotted to scrutinize the main atomic contributions and tells the possible sites of electronic transfer in which atoms are located. In all these energy-optimized structures (**Figure. 7**), phenothiazine employed a puckered butterfly structure. The HOMO lobes are distributed mostly over phenothiazine ring; whereas, the LUMO lobes are almost homogeneously spread over phenothiazine and terminal amine group somewhere. Based on the HOMO-LUMO energy gap, the MO theory of the chemical bond explains the concept of hard-soft molecules.<sup>50</sup> In the present study, all five compounds can be classified into a hard-molecule category and have good kinetic stability, as each of them shows large energy gap between HOMO and LUMO, i.e. ranging in between - 4.5 to - 4.9 eV.

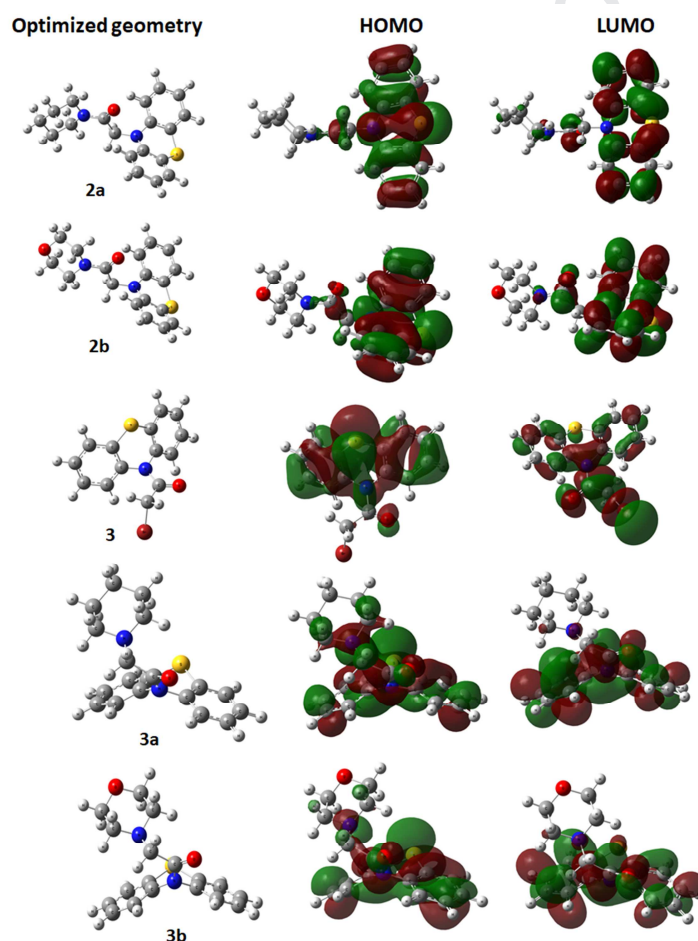


**Figure 7.** The optimized geometries and the surfaces of the frontier molecular orbital of compound **2a**, **2b**, **3**, **3a**, and **3b** obtained at the B3LYP/6-311++G(d,p).

Thus, this analysis shows that the HOMO-LUMO orbital is localized in the nearly same region of all compounds. Furthermore, the HOMO-LUMO energy gaps observed for all derivatives are seen to be nearly the same, thus suggesting that all five compounds exhibit nearly equivalent electronic structure properties.

**Table 4.** Energies of both HOMO and LUMO and their gaps (in eV) calculated for **2a**, **2b**, **3**, **3a** and **3b**

Compound	Energy (Hartee)	Dipole moments, $\mu$ (Debye)	HOMO (eV)	LUMO (eV)	HOMO-LUMO energy gap (eV)
<b>2a</b>	-1319.2632	5.4048	-5.1767	-0.6479	-4.5288
<b>2b</b>	-1355.16571	3.5179	-5.26486	-0.72899	-4.53587
<b>3</b>	-3642.02853	3.6014	-6.27849	-1.71786	-4.56063
<b>3a</b>	-1319.2525	2.934	-5.98351	-1.08002	-4.90349
<b>3b</b>	-1355.15645	3.3029	-6.10052	-1.18016	-4.92036

Electrostatic Potential Surface (ESP), the region provides a detailed description of both electron acceptor and electron donor areas.<sup>51</sup> The different colors signify the diverse values of ESP such as blue color represents the most positive electrostatic potential whereas red color represents the most electronegative electrostatic potential region. It also relates to the total charge distribution through dipole moment, partial charges, electronegativity, chemical reactivity sites of a compound. ESP offers a visual technique to comprehend the basic polarity of a molecule and acts as a valuable quantity to explain electrophilic and nucleophilic sites including hydrogen bonding, reactivity, and SAR (structure-activity relationship) of molecules including bio-molecules and drugs.

**Table 5.** Selected structural parameters by X-ray and theoretical calculations for all the compounds.

Bond lengths (Å)	Experimental	DFT/Theoretical	Bond angles (°)	Experimental (°)	DFT/Theoretical
<b>2a</b>					
C1A—C2A	1.386 (4)	1.394	C12A—C1A—C2A	120.5 (3)	120.8
C1A—C12A	1.384 (3)	1.400	C11A—N1A—C12A	120.27 (17)	120.48
C2A—C3A	1.373 (4)	1.391	C6A—S1A—C5A	98.83 (11)	99.05
<b>2b</b>					
C1A—C12A	1.382 (3)	1.400	C12A—C1A—C2A	121.1 (2)	120.84
C1A—C2A	1.383 (4)	1.394	C6A—S1A—C5A	100.07 (10)	99.06
O1A—C14A	1.214 (2)	1.220	C11A—N1A—C12A	122.01 (16)	120.52
S1A—C6A	1.743 (2)	1.782	C11A—N1A—C13A	117.25 (16)	119.38
N1A—C11A	1.390 (3)	1.414	C12A—N1A—C13A	118.36 (17)	119.43
N1A—C12A	1.401 (3)	1.414	C3A—C2A—C1A	120.4 (3)	120.5
<b>3</b>					
Br1A—C14A	1.951 (2)	1.979	C6A—S1A—C5A	98.32 (10)	97.99
S1A—C5A	1.771 (2)	1.787	C12A—N1A—C11A	115.52 (17)	115.70

S1A—C6A	1.767 (2)	1.783	C13A—N1A—C11A	123.42 (18)	124.90
O1A—C13A	1.223 (3)	1.214	C13A—N1A—C12A	120.21 (18)	118.58
N1A—C11A	1.442 (3)	1.434	C2A—C1A—H1A	119.4 (17)	120.80
N1A—C12A	1.430 (3)	1.437	C12A—C1A—H1A	120.5 (17)	119.43
<b>3a</b>					
C1—C2	1.382 (2)	1.392	C2—C1—C12	119.34 (14)	119.89
C1—C12	1.3919 (17)	1.395	C6—S1—C5	98.15 (5)	97.97
S1—C6	1.7573 (13)	1.782	C13—N1—C12	120.08 (10)	119.51
S1—C5	1.7629 (12)	1.787	C13—N1—C11	123.68 (10)	124.24
O1—C13	1.2209 (17)	1.216	C2—C1—C12	119.34 (14)	120.33
N1—C13	1.3729 (16)	1.398	C12—N1—C11	115.47 (9)	115.80
<b>3b</b>					
C1—C2	1.382 (2)	1.392	C2—C1—C12	119.34 (14)	119.87
C1—C12	1.3919 (17)	1.395	C6—S1—C5	98.15 (5)	97.97
S1—C6	1.7573 (13)	1.782	C13—N1—C12	120.08 (10)	119.42
S1—C5	1.7629 (12)	1.788	C13—N1—C11	123.68 (10)	124.29
O1—C13	1.2209 (17)	1.217	C12—N1—C11	115.47 (9)	115.76
N1—C13	1.3729 (16)	1.397	N2—C19—C18	111.35 (14)	109.87

The electrostatic potential surface (ESP) generated for these derivatives at B3LYP/6-311++G(d,p) level of theory, is shown in the supplementary **figure S13**. The ESP analysis of all derivatives shows that the nucleophilic sites are localized on carbonyl oxygen (C=O). Moreover, in the case of compounds **2b** and **3b**, the cyclic oxygen atom of (morpholine) is also observed to be an electron-rich region (nucleophile). Similarly, the electrophilic regions are concentrated near the aromatic hydrogen's of phenothiazine, in all compounds. Thus, the ESP analysis suggests that electrophilic and nucleophilic sites in all five derivatives of phenothiazine are nearly similar. We also conclude that the experimentally observed parameters such as bond lengths and bond angles for all five compounds were found to be in good agreement with the computed values. The theoretical structural and experimental data of the 10H substituted phenothiazine derivatives are listed in **Table 5**.

## Conclusion

The work includes synthesis, characterization, and crystal structure of five new 10H-substituted phenothiazine derivatives bearing alkyl chains (with two carbon chain lengths) and tertiary amino groups at the 10(H) position; subjected for the X-ray crystallography and DFT studies to evaluate their structural properties. Good qualities of single crystals suitable for X-ray diffraction analysis were obtained by recrystallization. The crystals were obtained in dichloromethane and tertiary butyl methyl ether solvents (1:1) at ambient temperature using the slow evaporation method. Our study identified that phenothiazine derivatives **2a** & **2b** crystallizes as the

Monoclinic, with space group  $P2_1/n$  and **3a** & **3b** crystallizes as the Monoclinic, with space group  $P2_1/c$  respectively. Compound **3** crystallized as orthorhombic with  $Pca2_1$ . The C–O···H and C–H···O hydrogen bond interactions, along with other weak interactions, stabilize the crystal packing. The purpose of the study was to analyze the consequence of the dissimilar crystal conformations of phenothiazine derivatives. In this connection, we compare the experimental and theoretical results of 10H-substituted phenothiazine derivatives. The HOMO–LUMO gap implies that these compounds have good kinetic stability and a high chemical reactivity whereas ESP gives the information on charge density distribution. Moreover, the computational study also suggests that all five derivatives of phenothiazine show nearly similar electronic structure properties such as electrophilic and nucleophilic sites and regions of HOMO and LUMO orbital localization.

#### Conflicts of interest

There are no conflicts of interest to declare.

#### Supporting Information

Supporting information includes the following

1. NMR ( $^1\text{H}$  and  $^{13}\text{C}$ ) of all reported compounds
2. Mass data of synthesized compounds
3. Crystal packing figures
4. Powder XRD pattern of the reported compounds

#### Acknowledgements

The authors would like to acknowledge the Indian Institute of Technology Gandhinagar for laboratory facilities and DST-FIST Department of Science and Technology, India for Single Crystal X-ray Diffraction Facility provided at IIT Gandhinagar (Project No. SR/FST/CSI-277/2016). The authors would also express sincere thanks to DRDO for funding.

#### References:

- 1 J. J. H. McDowell, *Acta Crystallogr. Sect. B*, 1976, **32**, 5–10.
- 2 T. A. Ban, *Neuropsychiatr. Dis. Treat.*, 2007, **3**, 495–500.
- 3 A. Bernthsen, *Berichte der Dtsch. Chem. Gesellschaft*, 1883, **16**, 1025–1028.
- 4 C. O. Okafor, *Dye. Pigment.*, 1986, **7**, 249–287.
- 5 F. DeEds and J. O. Thomas, *J. Parasitol.*, 1942, **28**, 363–367.

- 6 S. P. Massie, *Chem. Rev.*, 1954, **54**, 797–833.
- 7 W. E. Swales, *Can. J. Comp. Med.*, 1939, **3**, 188–194.
- 8 H. Maurer and K. Pflieger, *Arch. Toxicol.*, 1988, **62**, 185–191.
- 9 J. B. Mocko, A. Kern, B. Moosmann, C. Behl and P. Hajieva, *Neurobiol. Dis.*, 2010, **40**, 120–129.
- 10 J. N. Domínguez, S. López, J. Charris, L. Iarruso, G. Lobo, A. Semenov, J. E. Olson and P. J. Rosenthal, *J. Med. Chem.*, 1997, **40**, 2726–2732.
- 11 R. W. Wrenn, N. Katoh, R. C. Schatzman and J. F. Kuo, *Life Sci.*, 1981, **29**, 725–733.
- 12 J. E. Kristiansen and I. Mortensen, *Pharmacol. Toxicol.*, 1987, **60**, 100–103.
- 13 M. Viveiros and L. Amaral, *Int. J. Antimicrob. Agents*, 2001, **17**, 225–228.
- 14 P. Ratnakar, S. P. Rao, P. Sriramarao and P. S. Murthy, *Int. Clin. Psychopharmacol.*, 1995, **10**, 39–44.
- 15 H. Prinz, B. Chamasmani, K. Vogel, K. J. Böhm, B. Aicher, M. Gerlach, E. G. Günther, P. Amon, I. Ivanov and K. Müller, *J. Med. Chem.*, 2011, **54**, 4247–4263.
- 16 G. P. Sarmiento, R. G. Vitale, J. Afeltra, G. Y. Moltrasio and A. G. Moglioni, *Eur. J. Med. Chem.*, 2011, **46**, 101–105.
- 17 H. O. Strange, J. J. McGrath and J. P. Pellegrini, *I&EC Prod. Res. Dev.*, 1967, **6**, 33–35.
- 18 N. Manav, V. Verma, V. Pandey, H. Rather, R. Vasita and I. Gupta, *Indian J. Chem. - Section B*, 2019, **58**, 238–246.
- 19 J. M. Ford, W. C. Prozialeck and W. N. Hait, *Mol. Pharmacol.*, 1989, **35**, 105–115.
- 20 S. Ronald, S. Awate, A. Rath, J. Carroll, F. Galiano, D. Dwyer, H. Kleiner-Hancock, J. M. Mathis, S. Vigod and A. De Benedetti, *Genes and Cancer*, 2013, **4**, 39–53.
- 21 D. Tiwari, S. S. Thakkar and A. Ray, *Indian J. Chem.*, 2018, **57B**, 1194–1202.
- 22 V. Singh, P. K. Jaiswal, I. Ghosh, H. K. Koul, X. Yu and A. De Benedetti, *Cancer Lett.*, 2019, **453**, 131–141.
- 23 J. J. McKinnon, A. S. Mitchell and M. A. Spackman, *Chem. – A Eur. J.*, 1998, **4**, 2136–2141.
- 24 M. A. Spackman and J. J. McKinnon, *CrystEngComm*, 2002, **4**, 378–392.
- 25 J. J. McKinnon, D. Jayatilaka and M. A. Spackman, *Chem. Commun.*, 2007, 3814–3816.
- 26 G. M. Sheldrick, *Acta Crystallogr. Sect. A*, 2008, **64**, 112–122.
- 27 G. M. Sheldrick, *Acta Crystallogr. Sect. C*, 2015, **71**, 3–8.

- 28 C. F. Macrae, P. R. Edgington, P. McCabe, E. Pidcock, G. P. Shields, R. Taylor, M. Towler and J. van de Streek, *J. Appl. Crystallogr.*, 2006, **39**, 453–457.
- 29 C. R. Groom, I. J. Bruno, M. P. Lightfoot and S. C. Ward, *Acta Crystallogr. Sect. B*, 2016, **72**, 171–179.
- 30 F. H. Allen, *Acta Crystallogr. Sect. B*, 2002, **58**, 380–388.
- 31 I. J. Bruno, J. C. Cole, P. R. Edgington, M. Kessler, C. F. Macrae, P. McCabe, J. Pearson and R. Taylor, *Acta Crystallogr. B.*, 2002, **58**, 389–397.
- 32 J. J. McKinnon, M. A. Spackman and A. S. Mitchell, *Acta Crystallogr. B.*, 2004, **60**, 627–668.
- 33 M. A. Spackman and D. Jayatilaka, *CrystEngComm*, 2009, **11**, 19–32.
- 34 M. Toşa, C. Paizs, C. Majdik, L. Poppe, P. Kolonits, I. A. Silberg, L. Novák and F. D. Irimie, *Heterocycl. Commun.*, 2001, **7**, 277–282.
- 35 M. del Carmen Apreada, F. H. Cano, C. Foces-Foces, F. López-Rupérez, J. C. Conesa and J. Soria, *J. Chem. Soc. {,} Perkin Trans. 2*, 1987, 575–579.
- 36 L. J. Farrugia, *J. Appl. Crystallogr.*, 2012, **45**, 849–854.
- 37 E. Ramachandran and R. Dhamodharan, *J. Mater. Chem. C*, 2015, **3**, 8642–8648.
- 38 A. P. and G. B. Alexandru Turza, Maria O. Miclăuş, *Zeitschrift für Krist. - Cryst. Mater.*, 2019, 234, 671–683.
- 39 A. Turza, A. Pop, M. Muresan-Pop, L. Zarbo and G. Borodi, *J. Mol. Struct.*, 2020, **1199**, 126973.
- 40 Q. Hu, Y.-H. Yue, L.-Q. Chai and L.-J. Tang, *J. Mol. Struct.*, 2019, **1197**, 508–518.
- 41 V. R. Pedireddi, D. S. Reddy, B. S. Goud, D. C. Craig, A. D. Rae and G. R. Desiraju, *J. Chem. Soc. Perkin Trans. 1*, 1994, 2353–2360.
- 42 J. J. Koenderink and A. J. van Doorn, *Image Vis. Comput.*, 1992, **10**, 557–564.
- 43 N. H. H. Hassan, A. A. Abdullah, S. Arshad, N. C. Khalib and I. A. Razak, *Acta Crystallogr. Sect. E Crystallogr. Commun.*, 2016, **72**, 716–719.
- 44 M. J. Frisch, G. W. Trucks, H. B. Schlegel, G. E. Scuseria, M. a. Robb, J. R. Cheeseman, J. a. Montgomery, T. Vreven, K. N. Kudin, J. C. Burant, J. M. Millam, S. S. Iyengar, J. Tomasi, V. Barone, B. Mennucci, M. Cossi, G. Scalmani, N. Rega, G. a. Petersson, H. Nakatsuji, M. Hada, M. Ehara, K. Toyota, R. Fukuda, J. Hasegawa, H. Ishida, T. Nakajima, Y. Honda, O. Kitao, H. Nakai, M. Klene, X. Li, J. E. Knox, H. P. Hratchian, J.

- B. Cross, C. Adamo, J. Jaramillo, R. Gomperts, R. E. Stratmann, O. Yazyev, A. J. Austin, R. Cammi, C. Pomelli, J. Ochterski, P. Y. Ayala, K. Morokuma, G. a. Voth, P. Salvador, J. J. Dannenberg, V. G. Zakrzewski, S. Dapprich, A. D. Daniels, M. C. Strain, O. Farkas, D. K. Malick, A. D. Rabuck, K. Raghavachari, J. B. Foresman, J. V. Ortiz, Q. Cui, A. G. Baboul, S. Clifford, J. Cioslowski, B. B. Stefanov, G. Liu, A. Liashenko, P. Piskorz, I. Komaromi, R. L. Martin, D. J. Fox, T. Keith, M. a. Al-Laham, C. Y. Peng, A. Nanayakkara, M. Challacombe, P. M. W. Gill, B. Johnson, W. Chen, M. W. Wong, C. Gonzalez and J. a. Pople, *an Introd. To Comput. Chem. Using G09W Avogadro Softw.*
- 45 M. J. Frisch, G. W. Trucks, H. B. Schlegel, G. E. Scuseria, M. A. Robb, J. R. Cheeseman, J. A. Montgomery, T. Vreven, K. N. Kudin, J. C. Burant, J. M. Millam, S. S. Iyengar, J. Tomasi, V. Barone, B. Mennucci, M. Cossi, G. Scalmani, N. Rega, G. A. Petersson, H. Nakatsuji, M. Hada, M. Ehara, K. Toyota, R. Fukuda, J. Hasegawa, H. Ishida, T. Nakajima, Y. Honda, O. Kitao, H. Nakai, M. Klene, X. Li, J. E. Knox, H. P. Hratchian, J. B. Cross, C. Adamo, J. Jaramillo, R. Gomperts, R. E. Stratmann, O. Yazyev, A. J. Austin, R. Cammi, C. Pomelli, J. Ochterski, P. Y. Ayala, K. Morokuma, G. A. Voth, P. Salvador, J. J. Dannenberg, V. G. Zakrzewski, S. Dapprich, A. D. Daniels, M. C. Strain, O. Farkas, D. K. Malick, A. D. Rabuck, K. Raghavachari, J. B. Foresman, J. V. Ortiz, Q. Cui, A. G. Baboul, S. Clifford, J. Cioslowski, B. B. Stefanov, G. Liu, A. Liashenko, P. Piskorz, I. Komaromi, R. L. Martin, D. J. Fox, T. Keith, M. A. Al-Laham, C. Y. Peng, A. Nanayakkara, M. Challacombe, P. M. W. Gill, B. Johnson, W. Chen, M. W. Wong, C. Gonzalez and J. A. Pople, *G09W Tutorial*, 2009.
- 46 K. Fukui, T. Yonezawa and H. Shingu, *J. Chem. Phys.*, 1952, **20**, 722–725.
- 47 M. Saranya, S. Ayyappan, R. Nithya, R. K. Sangeetha and A. Gokila, *Dig. J. Nanomater. Biostructures*, 2018, **13**, 97–105.
- 48 S. Tripathy and S. Kumar Sahu, *J. PeerScientist*, 2018, **1**, 1–7.
- 49 N. Islam and S. Kaya, *Org. Med. Chem. Int. J.*, 2017, **2**, 555596.
- 50 R. G. Pearson, *J. Am. Chem. Soc.*, 1985, **107**, 6801–6806.
- 51 P. A. Wood, J. J. McKinnon, S. Parsons, E. Pidcock and M. A. Spackman, *CrystEngComm*, 2008, **10**, 368–376.

## **Synthesis and characterization of a new class of phenothiazine molecules with 10H-substituted morpholine & piperidine derivatives: A structural insight**

Javeena Hussain<sup>1</sup>, Deekshi Angira<sup>1</sup>, Tanya Hans<sup>1</sup>, Pankaj Dubey<sup>1</sup>, Sivapriya Kirubakaran<sup>1</sup> and  
Vijay Thiruvengatam<sup>2, \*</sup>

<sup>1</sup>Discipline of Chemistry, Indian Institute of Technology Gandhinagar, Gandhinagar, Gujarat-382355, India

<sup>2</sup>Discipline of Biological Engineering, Indian Institute of Technology Gandhinagar, Gandhinagar, Gujarat-382355, India  
E-mail: [vijay@iitgn.ac.in](mailto:vijay@iitgn.ac.in)

### **Highlights:**

- A new series of 10H-substituted phenothiazine derivatives have been crystallized.
- Interactions in crystal packing were supported by Hirshfeld surface and 2D-Fingerprint plot analysis.
- The crystal structure was investigated using DFT and the nature of HOMO and LUMO was theoretically studied.
- DFT study supports the formation of intermolecular hydrogen bonds and electrostatic interactions.
- Theoretical studies were performed with B3LYP/6-311++G(d,p) level to compare the best correlation of both theoretical with experimental data.

**Declaration of interests**

The authors declare that they have no known competing financial interests or personal relationships that could have appeared to influence the work reported in this paper.

The authors declare the following financial interests/personal relationships which may be considered as potential competing interests: